

Real-Time Optimization of a Hydroelectric Power Plant

M. Kiehl and O. von Stryk, München

Dedicated to the memory of Prof. Dr. Hansjörg Wacker

Received February 17, 1992; revised August 6, 1992

Abstract — Zusammenfassung

Real-Time Optimization of a Hydroelectric Power Plant. An optimal control problem modelling a hydroelectric power plant was developed and discussed by Hj. Wacker and his co-workers in [1]. In the present paper, this problem is treated within a more general framework of “non-differentiable” optimal control problems. Necessary conditions of optimality are derived and it is proven that the restricted class of controls considered in [1] indeed contains the optimal control. Furthermore, a decoupling technique is established that allows the full problem to be split into several small subproblems. Based on the new results, an efficient algorithm is developed. This algorithm allows the optimal control to be computed for more general problems with greater accuracy and for a longer time period. Numerical results are given both for the model described in [1] and for the more refined model presented in this paper.

AMS Subject Classifications: 49-04, 49K15, 65K10

Key words: Non-differentiable optimal control, singular control, hydroelectric power plant, real-time optimization.

Echtzeit-Optimierung eines Tagesspeicherkraftwerkes. Hj. Wacker und seine Mitarbeiter entwickelten und untersuchten das Modell eines Tagesspeicherkraftwerkes [1]. Bei der Optimierung der Energieausbeute beschränkten sie die Steuerung auf eine spezielle Funktionenklasse. Hier wird das Modell innerhalb einer verallgemeinerten Problemstellung behandelt. Die Optimierungsprobleme weisen Nichtdifferenzierbarkeiten in den Modellfunktionen auf, für die verallgemeinerte notwendige Optimalitätsbedingungen hergeleitet werden. Es wird nachgewiesen, daß die in [1] untersuchte Klasse die optimale Steuerung enthält und es werden Bedingungen hergeleitet, unter denen das Steuerungsproblem in Teilprobleme zerfällt. Darauf aufbauend wird ein effizienter Algorithmus beschrieben, der es erlaubt, in Echtzeit optimale Steuerungen auch für sehr lange Zeiträume mit hoher Genauigkeit zu berechnen. Numerische Ergebnisse werden für das Modell in [1] und eine Verallgemeinerung dieses Modells präsentiert.

1. The Modelling of the System

1.1 The General Model

The “day-storage” power plant model to be investigated is closely related to the Schwarzach Werk that was originally described by Hj. Wacker and his group in [1] and [12].

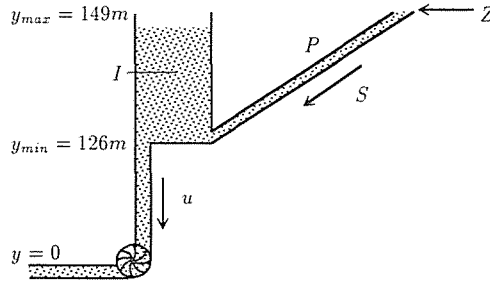


Figure 1

The plant operates like this: The water reservoir of the power plant is filled from the river Salzach using a pipeline P with an influx rate S . The rate S is constrained by the capacity W of the pipeline and the water influx $Z(t)$ to the pipeline. W depends on the difference of the pressure of water between both ends of the pipeline and therefore on the filling level y of the reservoir. Therefore, the actual influx of water in the storage through the pipeline is given by

$$S(y, t) = \min\{Z(t), W(y)\}. \quad (1)$$

The function $I(y)$ describes the relation between y and the contents of the storage. The control u is the flow of water through all turbines at time t and the function $\omega(u, y)$ is the efficiency. Following [1], the maximization of the energy production of the power plant over a period of one day, when the influx of water $Z(t)$ is known, can be described as the optimal control problem

$$\min_{u, y(0)} -g \int_0^T y(t)u(t)\omega(u(t), y(t)) dt, \quad g = 9.81[\text{kgm/s}^2], \quad T = 24[\text{h}], \quad (2)$$

subject to the dynamic equation

$$\dot{y}(t) = (S(y(t), t) - u(t)) \frac{\partial I(y)}{\partial y} \quad (3)$$

with boundary conditions

$$y(0) = y(T), \quad T = 24[\text{h}], \quad (4)$$

and the restrictions

$$y_{\min} := 126[\text{m}] \leq y(t) \leq 149[\text{m}] =: y_{\max}, \quad (5)$$

$$0 \leq u(t) \leq 107[\text{m}^3/\text{s}]. \quad (6)$$

1.2 The Three-Peak Model

In the so-called three-peak model the hitherto unspecified functions can be found in [1]. The contents I of the reservoir is assumed to be a linear function of the filling level y

$$I(y) = \alpha(y - 126)[\text{m}^3], \quad (7)$$

$$\frac{\partial I}{\partial y} = \alpha = \frac{1.48}{23} 10^6 [\text{m}^2]. \quad (8)$$

The linear function I reflects the cylindrical geometry of the storage. The energy production depends on the water pressure and the water volume u which flows through the downpipe to the power plant and is assumed to be proportional to the potential energy with the constant of proportionality (i.e. the efficiency factor)

$$\omega(u, y) = \text{const.} \quad (9)$$

Setting $\omega(u, y) \equiv 1$ the objective function then becomes

$$\min \int_0^T (-y(t)u(t)) dt. \quad (10)$$

The capacity $W(y)$ of the pipeline is assumed to be linear

$$W(y) = 80 \left(1 - \frac{y - 126}{23} \right) \left[\frac{\text{m}^3}{\text{s}} \right], \quad (11)$$

and the water influx $Z(t)$ is a given periodic function with a period of one day and the constraint $20 \leq Z \leq 40 [\text{m}^3/\text{s}]$. Here, the influx is approximated by the step function

$$Z(t) = \begin{cases} 40 [\text{m}^3/\text{s}], & \text{if } t \in [T_1, T_2] \vee [T_3, T_4] \vee [T_5, T_6], \\ 20 [\text{m}^3/\text{s}], & \text{elsewhere} \end{cases} \quad (12)$$

with $(T_1, T_2, T_3, T_4, T_5, T_6) := (8\text{h}, 10\text{h}, 13\text{h}, 15\text{h}, 18\text{h}, 20\text{h})$. Following [1], we shall call this model the three-peak model.

1.3 A Refined Three-Peak Model

In the present paper, a refinement of the three-peak model is suggested. The refined model is nonlinear and describes some physical effects more realistically than in [1].

1. The influx of water is described by a piecewise cubic polynomial $Z_R(t)$ being a continuously differentiable function with respect to the time t .

$$Z_R(t) = \begin{cases} 20 [\text{m}^3/\text{s}], & \text{if } t \in [0\text{h}, 7.75\text{h}], \\ 20(2 + 2(2(8.25 - t))^3 - 3(2(8.25 - t))^2) [\text{m}^3/\text{s}], & \text{if } t \in [7.75\text{h}, 8.25\text{h}], \\ 40 [\text{m}^3/\text{s}], & \text{if } t \in [8.25\text{h}, 9.75\text{h}], \\ 20(2 + 2(2(t - 9.75))^3 - 3(2(t - 9.75))^2) [\text{m}^3/\text{s}], & \text{if } t \in [9.75\text{h}, 10.25\text{h}], \\ 20 [\text{m}^3/\text{s}], & \text{if } t \in [10.25\text{h}, 13.75\text{h}], \\ \text{etc.} & \end{cases} \quad (13)$$

Comparing both models, note that $Z_R(t)$ is related to the original $Z(t)$ by

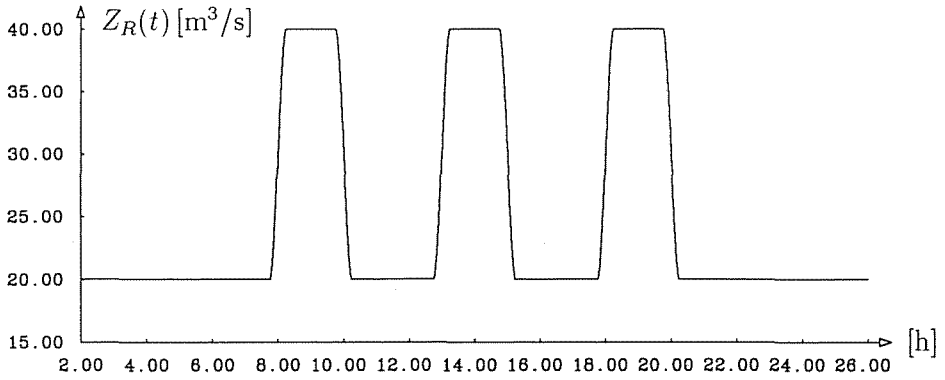


Figure 2

$$\int_0^T Z_R(t) dt = \int_0^T Z(t) dt. \quad (14)$$

Every known influx can be sufficiently well approximated by piecewise cubic polynomials.

2. The reservoir is assumed to have the geometry of a truncated cone

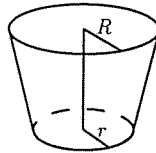


Figure 3

with $\rho := R/r \geq 1$; in the numerical calculations the choice was $\rho = 1.25$. The function $I_R(y)$ is a cubic polynomial satisfying $I_R(y_{\max}) = 1.48 \cdot 10^6 =: I_{\max}$ and $I_R(y_{\min}) = 0$. Therefore

$$I_R(y) = \frac{I_{\max}}{1 + \rho + \rho^2} \hat{y} (3 + 3(\rho - 1)\hat{y} + (\rho - 1)^2 \hat{y}^2) \quad (15)$$

where

$$\hat{y} = \frac{y - y_{\min}}{y_{\max} - y_{\min}} = \frac{y - 126}{23}. \quad (16)$$

For $\rho = R/r = 1$, we have $I_R(y) = I(y)$ and for $\rho > 1$, we may write $I_R(y)$ as

$$I_R(y) = \frac{I_{\max}}{\rho^3 - 1} \left(\left(1 + (\rho - 1) \frac{y - 126}{23} \right)^3 - 1 \right) \quad (17)$$

and

$$\frac{\partial I_R}{\partial y} = \frac{I_{\max}}{1 + \rho + \rho^2} \frac{3}{23} \left(1 + (\rho - 1) \frac{y - 126}{23} \right)^2, \quad \rho \geq 1. \quad (18)$$

The denominator of the dynamic equation (3) is $\partial I_R / \partial y$. The zeros are of special interest.

$$\frac{\partial I_R}{\partial y} = 0 \Leftrightarrow y_{1,2} - 126 = -\frac{23}{\rho - 1} \quad \text{where} \quad y_{1,2} - 126 < 0. \quad (19)$$

Due to the restrictions on y , this case cannot happen.

3. A modification of $W(y)$, already suggested in [1], is taken into account

$$W_R(y) = 80 \left(1 - \left(\frac{y - 126}{23} \right)^2 \right) \left[\frac{m^3}{s} \right]. \quad (20)$$

2. Necessary Conditions for Singular Controls

2.1 Optimal Control Problems when the Dimension of the State Equals the Dimension of the Control

In view of the problems of Sec. 1, we now assume that the control u and the state variable y are of the same dimension. In this case we can expect that the system is totally controllable if the constraints on the control u are not active. The first-order necessary conditions are derived as follows. Let us consider an optimal control problem

$$J := \min_u \int_a^b L(y(t), u(t), t) dt \quad (21)$$

subject to a system of differential equations

$$\dot{y}(t) = g(y(t), u(t), t) \quad (22)$$

where $y = (y_1, \dots, y_n)^T$, $u = (u_1, \dots, u_n)^T$, $L: \mathbb{R}^n \times \mathbb{R}^n \times \mathbb{R} \rightarrow \mathbb{R}$ and $g: \mathbb{R}^n \times \mathbb{R}^n \times \mathbb{R} \rightarrow \mathbb{R}^n$. L and g are assumed to be a.e. continuously differentiable. With

$$F := L + \lambda^T(t)(g - \dot{y}), \quad \lambda = (\lambda_1, \dots, \lambda_n)^T, \quad (23)$$

the necessary first-order conditions for an optimal trajectory $(y(t), u(t))$ are (cf. Hestenes [7])

$$\frac{d}{dt} F_y - F_y = -\dot{\lambda}^T - L_y - \lambda^T g_y = 0 \quad \text{a.e. in } [a, b] \quad (24)$$

and, if F is nonlinear in u_i , we have

$$-F_{u_i} = -L_{u_i} - \lambda^T g_{u_i} = 0 \quad \text{a.e. in } [a, b]. \quad (25)$$

If F is linear in u_i and if u_i is constrained by $u_{\min, i} \leq u_i \leq u_{\max, i}$, the minimum principle yields

$$u_i = \begin{cases} u_{\max,i}, & \text{if } F_{u_i} < 0, \\ u_{\min,i}, & \text{if } F_{u_i} > 0, \\ \text{singular}, & \text{if } F_{u_i} = 0. \end{cases} \quad (26)$$

If the Jacobian $g_u := (\partial g_i / \partial u_j)_{i,j=1}^n$ is regular, we obtain

$$\lambda^T = -L_u g_u^{-1} \quad (27)$$

from (25) and (26) no matter whether F is nonlinear in u or both linear in u and singular. In these two cases, the parameter λ can be eliminated from (24) which yields

$$\sigma(u, y, t) := \frac{d}{dt}(L_u g_u^{-1}) - L_y + L_u g_u^{-1} g_y = 0 \quad \text{a.e. in } [a, b] \quad (28)$$

with $\sigma: \mathbb{R}^n \times \mathbb{R}^n \times \mathbb{R} \rightarrow \mathbb{R}^n$.

Lemma 1. *Let $n = 1$ and $g, L: \mathbb{R} \times \mathbb{R} \times \mathbb{R} \rightarrow \mathbb{R}$ be a.e. three times continuously differentiable with $g_u \neq 0$. If $(L_u g_u^{-1})_u = 0$ for all (y, u) in a time interval where the optimal control is not constrained, then the function σ is independent of u*

$$\sigma = \sigma(y, t) = 0. \quad (29)$$

Note that $(L_u g_u^{-1})_u = 0$ is satisfied if g and L are linear in u . The assumptions of Lemma 1 are therefore fulfilled for the problems of Sec. 1.

Proof: With $\dot{y} = g$ we obtain from (28)

$$\sigma = \sigma(u, y, t) = (L_u g_u^{-1})_y g + (L_u g_u^{-1})_t - L_y + (L_u g_u^{-1}) g_y = 0 \quad (30)$$

and

$$\begin{aligned} \frac{\partial \sigma(u, y, t)}{\partial u} &= (L_u g_u^{-1})_{yu} g + (L_u g_u^{-1})_y g_u + (L_u g_u^{-1})_{ut} - L_{yu} + (L_u g_u^{-1})_{u} g_y + (L_u g_u^{-1}) g_{yu} \\ &\equiv \frac{\partial}{\partial y} (L_u g_u^{-1} g_u - L_u) \equiv 0. \end{aligned} \quad (31)$$

As a consequence $\sigma(u, y, t)$ does not depend on u . ■

2.2 First-Order Necessary Conditions

The first-order conditions can be written as follows. Defining the Hamiltonian H as $H := L + \lambda^T g$, Eq. (24) now becomes the adjoint differential equations

$$\dot{\lambda}_i = -H_{y_i}, \quad i = 1, \dots, n. \quad (32)$$

The optimal control u has to satisfy the minimum principle. If H is linear in u_i and if u_i is constrained, we have

$$u_i = \begin{cases} u_{\max,i}, & \text{if } H_{u_i} < 0, \\ u_{\min,i}, & \text{if } H_{u_i} > 0, \\ \text{singular}, & \text{if } H_{u_i} \equiv 0. \end{cases} \quad (33)$$

On singular subarcs, we also have $dH_{u_i}/dt \equiv 0$.

Application: For the models of the power plant considered in Sec. 1, the Hamiltonian is $H = L + \lambda^T g = -yu + \lambda g$ with $L(y, u, t) = -yu$ and $\dot{y} = g(y, u, t) = (S(y, t) - u)/I_y(y)$. The adjoint variable λ satisfies

$$\dot{\lambda} = -H_y = u - \lambda \frac{S_y(y, t)I_y(y) - I_{yy}(y)(S(y, t) - u)}{(I_y(y))^2}. \quad (34)$$

On singular subarcs, we therefore find from $H_u \equiv 0$, $y = -\lambda/I_y(y)$ and

$$0 \equiv \frac{d}{dt}H_u = -\dot{y} - \frac{\dot{\lambda}I_y - \lambda I_{yy}\dot{y}}{(I_y)^2} \quad (35)$$

$$= -\frac{S - u}{I_y} - (I_y)^{-1} \left(u - \lambda \frac{S_y I_y - I_{yy}(S - u)}{(I_y)^2} \right) + \frac{I_{yy}}{(I_y)^2} \lambda \frac{S - u}{I_y} \quad (36)$$

$$= (I_y)^{-1}(-S - yS_y). \quad (37)$$

In addition, on singular subarcs we have with (28)

$$\sigma = \frac{d}{dt}(L_u g_u^{-1}) - L_y + L_u g_u^{-1} g_y \quad (38)$$

$$= \frac{d}{dt}(yI_y) + u + \frac{S_y I_y - (S - u)I_{yy}}{(I_y)^2} yI_y \quad (39)$$

$$= S + yS_y \equiv 0. \quad (40)$$

•

In general, i.e. for $n \geq 1$, H_u and σ are related to each other, due to Eqs. (24), (27), and (28), via

$$\frac{d}{dt}(H_u g_u^{-1}) = \frac{d}{dt}((L_u + \lambda^T g_u)g_u^{-1}) \quad (41)$$

$$= \frac{d}{dt}(L_u g_u^{-1}) - L_y - \lambda^T g_y \quad (42)$$

$$= \frac{d}{dt}(L_u g_u^{-1}) - L_y + L_u g_u^{-1} g_y \quad (43)$$

$$= \sigma(u, y, t). \quad (44)$$

Application: In the models considered in Sec. 1, L and g are linear in u , and $g_u \neq 0$. Assuming that $Z(t) - W(y(t))$ has only isolated zeros along the optimal trajectory, two cases have to be distinguished for the above mentioned necessary condition (40) for a singular control.

1st case: $S = Z(t)$ holds and we have

$$\sigma = Z(t) + y \cdot 0 \neq 0 \quad (45)$$

since $20 \leq Z(t) \leq 40$. Hence, σ has no zero when $S = Z(t)$.

2nd case: $S = W(y)$ holds and we have

$$\sigma = W(y) + yW_y(y). \quad (46)$$

For the three-peak model we have

$$\sigma = (149 - y)\frac{80}{23} + y\left(-\frac{80}{23}\right) = 0 \Leftrightarrow y = 74.5. \quad (47)$$

Due to the restriction $126 \leq y \leq 149$, this filling level y is not feasible.

In the refined three-peak model we have

$$\sigma = 80\left(1 - \left(\frac{y - 126}{23}\right)^2\right) + y(-2)\frac{y - 126}{23} \cdot \frac{80}{23} = 0 \quad (48)$$

$$\Leftrightarrow y_1 = 128.049 \dots \quad \text{or} \quad y_2 = 39.950 \dots \quad (49)$$

Although y_1 is feasible with respect to the constraints, this filling level 128.049 is not reached as we shall see later on. According to the classical theory, singular subarcs cannot occur as long as all functions appearing in the problem are differentiable. However, this is not true here along the curve $y(t) = y^*(t)$ defined by $W(y^*(t)) = Z(t)$. Along this special trajectory the influx S switches between $Z(t)$ and $W(y)$. As it will be shown in the following, the optimal filling level y indeed becomes

$$y(t) = y^*(t) = W^{-1}(Z(t)) \quad (50)$$

within several subintervals. So we have to derive necessary conditions for the more general case when L and g may be non-differentiable. \bullet

2.3 More General Necessary Conditions

Theorem 1. Let $\eta_0: \mathbb{R} \rightarrow \mathbb{R}^n$ be the optimal solution of the variational problem

$$\min_y J[y], \quad J[y] := \int_a^b L(y, \dot{y}, t) dt. \quad (51)$$

The functions $L: \mathbb{R}^n \times \mathbb{R}^n \times \mathbb{R} \rightarrow \mathbb{R}$ and $L_{\dot{y}}$ are assumed to be continuously differentiable in a neighborhood of $(\eta_0(t), \dot{\eta}_0(t), t)$, for all $t \in [a, b]$, with one exception: $\partial L/\partial y_i$ and $\partial L_{\dot{y}}/\partial y_i$ need not to exist for $y(t) = \eta_0(t)$. But then at least the one sided limits for $h \downarrow 0$ and $h \uparrow 0$ of $\partial L(\eta_0 + he_i, \dot{\eta}_0, t)/\partial y_i$ and $\partial L_{\dot{y}}(\eta_0 + he_i, \dot{\eta}_0, t)/\partial y_i$ are assumed to exist. Then, for $i = 1, \dots, n$, the following two necessary conditions hold

$$\begin{aligned} \lim_{h \downarrow 0} \left(\frac{d}{dt} L_{\dot{y}_i}(\eta_0 + he_i, \dot{\eta}_0, t) - L_{y_i}(\eta_0 + he_i, \dot{\eta}_0, t) \right) &\leq 0, \\ \lim_{h \uparrow 0} \left(\frac{d}{dt} L_{\dot{y}_i}(\eta_0 + he_i, \dot{\eta}_0, t) - L_{y_i}(\eta_0 + he_i, \dot{\eta}_0, t) \right) &\geq 0, \end{aligned} \quad (52)$$

where e_i is the i -th canonical unit vector.

Note that if $dL_{\dot{y}}(\eta, \dot{\eta}, t)/dt - L_{y_i}(\eta, \dot{\eta}, t)$ is continuous, Eq. (52) is equivalent to the well-known Euler-Lagrange equation.

Proof: Let $n = 1$. We use functions η_ε , $\varepsilon > 0$, with support on $[\alpha, \beta]$ and defined by

$$\eta_\varepsilon = \begin{cases} (t - \alpha)\varepsilon, & \text{if } \alpha < t < \alpha + \varepsilon, \\ \varepsilon^2, & \text{if } \alpha + \varepsilon \leq t \leq \beta - \varepsilon, \\ (\beta - t)\varepsilon, & \text{if } \beta - \varepsilon < t < \beta, \\ 0, & \text{otherwise.} \end{cases} \Rightarrow \dot{\eta}_\varepsilon = \begin{cases} \varepsilon, & \text{if } \alpha < t < \alpha + \varepsilon, \\ 0, & \text{otherwise,} \\ -\varepsilon, & \text{if } \beta - \varepsilon < t < \beta. \end{cases} \quad (53)$$

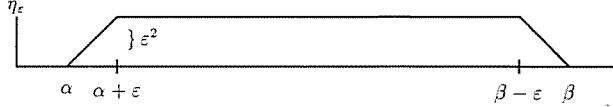


Figure 4

With suitable functions ζ between η_0 and $\eta_0 + \eta_\varepsilon$ and $\hat{\zeta}$ between $\dot{\eta}_0$ and $\dot{\eta}_0 + \dot{\eta}_\varepsilon$ and because $\dot{\eta}_\varepsilon \in \{-\varepsilon, 0, +\varepsilon\}$ and $\eta_\varepsilon \leq \varepsilon^2$, we have for all $\varepsilon \geq 0$

$$\begin{aligned} J[\eta_0 + \eta_\varepsilon] - J[\eta_0] &= \int_\alpha^\beta L_y(\zeta, \dot{\eta}_0, t) \eta_\varepsilon dt + \int_\alpha^{\alpha+\varepsilon} L_y(\eta_0, \hat{\zeta}, t) \dot{\eta}_\varepsilon dt \\ &\quad + \int_{\beta-\varepsilon}^\beta L_y(\eta_0, \hat{\zeta}, t) \dot{\eta}_\varepsilon dt + O(\varepsilon^3) \\ &= \varepsilon^2 \left(\int_\alpha^\beta L_y(\zeta, \dot{\eta}_0, t) dt \right) + \varepsilon \left(\int_\alpha^{\alpha+\varepsilon} L_y(\eta_0, \hat{\zeta}, t) dt \right) \\ &\quad - \varepsilon \left(\int_{\beta-\varepsilon}^\beta L_y(\eta_0, \hat{\zeta}, t) dt \right) + O(\varepsilon^3) \end{aligned} \quad (54)$$

$$\begin{aligned} &= \varepsilon^2 \left(\int_\alpha^\beta L_y(\zeta, \dot{\eta}_0, t) dt + L_y(\eta_0(\alpha), \hat{\zeta}(\alpha), \alpha) - L_y(\eta_0(\beta), \hat{\zeta}(\beta), \beta) \right) \\ &\quad + O(\varepsilon^3) \end{aligned} \quad (55)$$

$$\geq 0. \quad (56)$$

With $\varepsilon \rightarrow 0$ we obtain, for all $\alpha, \beta \in [a, b]$,

$$F(\alpha, \beta) := \int_\alpha^\beta L_y(\eta_0^+, \dot{\eta}_0, t) dt + L_y(\eta_0, \dot{\eta}_0, \alpha) - L_y(\eta_0, \dot{\eta}_0, \beta) \geq 0, \quad (57)$$

with $\eta_0^+(t) = \lim_{\varepsilon \downarrow 0} (\eta_0(t) + \eta_\varepsilon(t))$. Now we proceed as follows. Assume that $dL_y/dt - L_y > 0$ for $t = t_s \in [a, b]$, then choose $\alpha = \beta = t_s$ and find $F(t_s, t_s) = 0$, but $dF(t_s, t_s)/d\beta < 0$. Therefore $F(t_s, t_s + \delta) < 0$ for sufficiently small $\delta > 0$. Thus, the first inequality of Theorem 1 follows from the inequality $F(\alpha, \beta) \geq 0$ by contradiction. The second inequality is obtained by using $\eta_0 - \eta_\varepsilon$ as the competitive function.

The proof for $n > 1$ is straightforward by discussing each component of η_i separately. \blacksquare

If $g_u \in \mathbb{R}^{n \times n}$ is regular, Theorem 1 can be used for the problem (21) and (22) of Sec. 2.1 in all those intervals $]a_s, b_s[$ where the control is singular. This will be explained by

Theorem 2. Let $\eta_0, u_0: \mathbb{R} \rightarrow \mathbb{R}^n$ be the optimal solution of the optimal control problem

$$\min_u J[u], \quad J[u] := \int_a^b L(y, u, t) dt, \quad \text{s.t.} \quad \dot{y} = g(y, u, t). \quad (58)$$

The functions L , L_u , g , and g_u are assumed to be continuously differentiable except with respect to y for $y(t) = \eta_0(t)$ where only the one-sided limits are assumed to exist and $g_u \in \mathbb{R}^{n \times n}$ is assumed to be regular. Then, for $i = 1, \dots, n$, the following two necessary conditions hold on singular subarcs

$$\lim_{h \downarrow 0} \sigma_i(u_0, \eta_0 + h e_i, t) \leq 0 \leq \lim_{h \uparrow 0} \sigma_i(u_0, \eta_0 + h e_i, t). \quad (59)$$

Proof: If g_u is regular and if u is singular, it follows from $\dot{y} = g(y, u, t)$ that

$$u = G(y, \dot{y}, t) \Rightarrow I = G_y g_u \quad \text{and} \quad 0 = G_y + G_y g_y. \quad (60)$$

We find that $G_y = g_u^{-1}$ and $G_y = -g_u^{-1} g_y$.

Applying Theorem 1 to $L^*(y, \dot{y}, t) := L(y, G(y, \dot{y}, t), t)$, we obtain

$$\frac{d}{dt} L_y^* - L_y^* = \frac{d}{dt} \left(\frac{\partial(L(y, G(y, \dot{y}, t), t))}{\partial \dot{y}} \right) - \frac{\partial L(y, G(y, \dot{y}, t), t)}{\partial y} \quad (61)$$

$$= \frac{d}{dt} (L_u g_u^{-1}) - L_y + L_u g_u^{-1} g_y \quad (62)$$

$$= \sigma(u, y, t), \quad (63)$$

and Theorem 2 follows from Theorem 1. ■

If for all admissible u , we find y^* with $\sigma_i(u, y, t_s) > 0$ for all y with $y_i < y_i^*$ and $\sigma_i(u, y, t_s) < 0$ for all y with $y_i > y_i^*$, for all $i = 1, \dots, n$, then y^* is the only candidate for an optimal trajectory having a singular subarc. The associated singular control will be denoted by u^* . Consequently we can restrict u to the three values $u(t) \in \{u_{\min}, u_{\max}, u^*(t)\}$.

Application: In the problems considered in Sec. 1, $S = \min\{Z(t), W(y)\}$, and from (40) $\sigma(y) = S + y S_y$ satisfies the conditions of Eq. (59) of Theorem 2 for $\eta_0 = y^*$ since

$$y < y^* \Rightarrow S = Z(t) \Rightarrow \sigma(y) = Z(t) > 0 \quad (64)$$

and

$$y > y^* \Rightarrow \sigma(y) = W + y W_y < 0, \quad (65)$$

if $y > 74.5$ in the three-peak model,

or if $y > y_1 = 128.049\dots$ in the refined three-peak model.

A singular control can therefore exist only if $y = y^*$. ●

Eqs. (64) and (65) show that in the problems considered in Sec. 1 the inequality (59) is a strict inequality. Therefore, inequality (59) remains valid under small problem modifications.

2.4 Decoupling by Singular Subintervals

Decoupling Technique: Let the assumptions of Theorem 2 be valid with Eq. (59) determining $y^*(t)$ for all t . Let (u_{opt}, y_{opt}) be the unique solution of the optimal control problem

$$\min_u \int_a^b L(y, u, t) dt, \quad \text{s.t.} \quad \dot{y} = g(y, u, t). \quad (66)$$

Let u_{opt} be singular ($u_{opt} = u^*$) in the intervals $[t_1, t_2]$ and $[t_3, t_4]$, $t_2 < t_3$, and let (u_1, y_1) be the unique solution of the optimal control problem

$$\min_u \int_{t_1}^{t_4} L(y, u, t) dt, \quad \text{s.t.} \quad \dot{y} = g(y, u, t) \quad (67)$$

with the boundary conditions that $u(t_1)$ and $u(t_4)$ are singular.

Then by the Principle of Optimality, $(u_{opt}(t), y_{opt}(t)) = (u_1(t), y_1(t))$ for all $t \in [t_1, t_4]$.

If the optimal control is singular within several subintervals, certain subproblems can be solved separately over smaller time intervals and can be matched together resulting in an optimal solution for a longer time period. Of course, the intervals where the optimal control is singular have to be known in advance. In the following, we provide a strategy for finding candidates for singular subarcs and for demonstrating the validity of this assumption. The decoupling technique will significantly decrease the computing time as compared to the amount of computing time for the full problem.

In order to find the optimum u_1 , we only have to know the model functions, e.g., the influx $Z(t)$ to the hydroelectric reservoir mentioned in Sec. 1 for $t \in [t_1, t_4]$, for a short period in the future. For example, it is sufficient to know the influx of water $Z(t)$ or $Z_R(t)$, respectively, only about 5 hours in advance.

3. Application to the Hydroelectric Power Plant

3.1 Restriction of the Class of Admissible Controls

For the optimal control problems (21), we find under the assumptions of Theorem 2 that the optimal control $u(t)$ can only have 3 values, $u(t) = u_{\min}$, $u(t) = u_{\max}$, and $u(t) = u^*(t) = G(y^*(t), \dot{y}^*(t), t)$. The control u is determined by all switching points where u switches between two of these three values. We now show that the number and the type of these switching points can be limited. We then optimize only with respect to these few parameters.

Lemma 2. Let $t = t_b$ be a so-called **bang-bang** point where the control u switches between $u = u_{\max}$ and $u = u_{\min}$ or vice versa. Then

$$u = \begin{cases} u_{\max} & \text{for } t \in [t_b - \varepsilon, t_b[\\ u_{\min} & \text{for } t \in]t_b, t_b + \varepsilon] \end{cases} \Rightarrow y(t_b) \geq y^*(t_b) \tag{68}$$

or

$$u = \begin{cases} u_{\min} & \text{for } t \in [t_b - \varepsilon, t_b[\\ u_{\max} & \text{for } t \in]t_b, t_b + \varepsilon] \end{cases} \Rightarrow y(t_b) \leq y^*(t_b), \tag{69}$$

respectively, for a sufficiently small $\varepsilon > 0$.

Proof: (Indirect) 1st case only: Since $y(t)$ and $y^*(t)$ are continuous, we find

$$y(t_b) < y^*(t_b) \Rightarrow y(t) < y^*(t) \quad \text{for } t \in [t_b - \varepsilon, t_b + \varepsilon] \text{ with a sufficiently small } \varepsilon > 0. \tag{70}$$

As y and λ are continuous, $H_u = -y - \lambda/I_y(y)$ is also continuous with $H_u(t_b) = 0$. From (44), we find

$$[\sigma(y)]_{t \uparrow t_b} = \frac{d}{dt} [-I_y H_u]_{t \uparrow t_b} = [-I_{yy} \dot{y} H_u - I_y \dot{H}_u]_{t \uparrow t_b} = -I_y(y(t_b)) [\dot{H}_u]_{t \uparrow t_b}. \tag{71}$$

On the other hand, we see from (64) that $\sigma(y) = Z(t) > 0$ for $y < y^*$. With $I_y > 0$ it follows that $\dot{H}_u(t) < 0$ for $t \in [t_b - \delta, t_b[$ with a sufficiently small $\delta > 0$. Conclusively $H_u(t) > 0$ for $t \in [t_b - \delta, t_b[$, which contradicts $u = u_{\max}$ (because of (33)). ■

As a consequence, we have the result that after a switch from $u = u_{\max}$ to $u = u_{\min}$ —or vice versa—the next switching point cannot occur before $y - y^*$ has changed its sign. This severely restricts the number of switching points as we will see from Fig. 5.

For a given $Z(t)$, we calculate $y^* = W^{-1}(Z(t))$ and the associated singular control u^* from

$$u^*(t) = S(y^*, t) - \dot{y}^* I_y(y^*). \tag{72}$$

In Fig. 5 the solid line refers to y^* . The control u^* may violate the restrictions for u in some intervals, say $[\tau_{l,1}, t_{f,1}]$, $[\tau_{l,2}, t_{f,2}]$, ..., $[\tau_{l,m}, t_{f,m}]$; the graph of y^* is shown by a thin solid line.

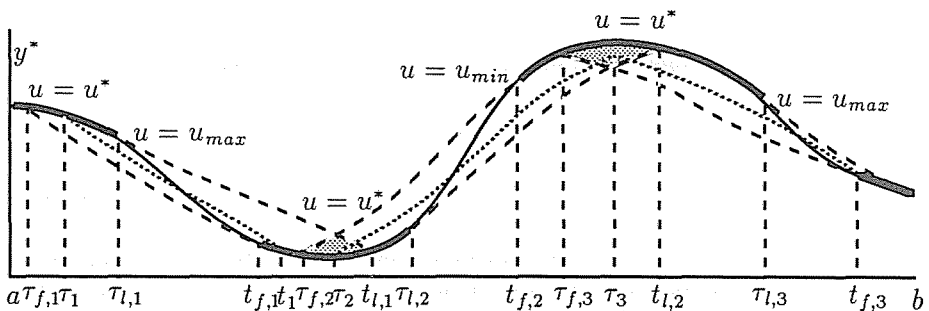


Figure 5

The control can be singular only in the intervals $[a, \tau_{i,1}]$, $[t_{f,1}, \tau_{i2}]$, etc., in Fig. 5; the graph of y^* is shown there by a bold solid line.

We now assume that the optimal control is singular at $t = a$ and $t = b$. Then u might be singular for $a \leq t < \tau_1$ with τ_1 the exit point of the first singular subarc which is to be determined. Obviously τ_1 is bounded by $\tau_1 \leq \tau_{i,1}$ where $\tau_{i,1}$ denotes the last possible exit point of the first singular subarc. In addition, τ_1 is bounded by $\tau_{f,1} \leq \tau_1$ where $\tau_{f,1}$ is the first possible exit point of the first singular subarc. After this point, u can switch from u^* to u_{\max} so that y can still hit the curve y^* .

In the following, we will distinguish between two types of switching points. The switching points where the control switches either to u_{\max} or u_{\min} are denoted by τ_i and the switching points where the control switches to u^* are denoted by t_i .

A possible optimal trajectory (dotted line) may hit the curve y^* at the point $t_1 := t_1(\tau_1)$ where u switches from u_{\max} to u^* . This switching point t_1 is bounded by $t_{f,1} \leq t_1 \leq t_{i,1}$. The point $t_{i,1}$ is defined by $t_{i,1} = t_{i,1}(\tau_{i,1})$, and $\tau_{f,1}$ can be computed by backward integration starting with $y(t_{f,1}) = y^*(t_{f,1})$ and $u = u_{\max}$ until the stopping condition $y(t) = y^*(t)$.

The optimal trajectory is therefore bounded in its first part by a tube between the two dashed lines, starting at $\tau_{f,1}$ and $\tau_{i,1}$, respectively, and the bold solid line segments. If u switches to u_{\min} at $t = \tau_2$, then, because of Lemma 1 the trajectory must be in the next tube, i.e., between the two dashed lines starting at $\tau_{f,2}$ and $\tau_{i,2}$. A bang-bang point, e.g., $t = \tau_3$, where the solid line segments of y^* are not met by the dotted line of y , can therefore only be located in the crosssection of the two tubes (dotted area).

The optimal control u can thus be described by the m switching points $\tau_1, \tau_2, \dots, \tau_m$ only. Note that the switching points t_i depend on τ_i and they exist only if $t_i < \tau_{i+1}$.

This is exactly what Bauer, Reisinger, and Wacker did in [1]. By the investigations of Sec. 2, it is now shown that the authors of [1] considered the correct set of possible control functions, although necessary conditions were not used in [1].

3.2 The State Constraint

Although the state constraint (5) of y never becomes active in the models considered, the results can be extended to problems with a boundary arc due to this constraint. This case can be treated by defining an additional constraint upon u ,

$$\bar{u} \begin{cases} \leq S(y, t), & \text{if } y = y_{\min}, \\ \geq S(y, t), & \text{if } y = y_{\max}, \end{cases} \quad (73)$$

and one can show that $u(t)$ becomes

$$u(t) = u_{\min} \quad \text{or} \quad u(t) = u_{\max} \quad \text{or} \quad u(t) = \bar{u}^*(t) = S(\bar{y}^*, t) - \dot{\bar{y}}^* I_y(\bar{y}^*) \quad (74)$$

with

$$\bar{y}^* := \min\{y_{\max}, \max\{y_{\min}, y^*\}\}. \quad (75)$$

Then we have to replace y^* by \bar{y}^* in the following algorithm.

4. Real Time Optimization Algorithm

The algorithm can be described by the following steps. The interval $[a, b]$ is the time period considered.

Step 1: Compute the number m of intervals $[\tau_{l,i}, t_{f,i}]$ for $i = 1, \dots, m$, where u^* violates the constraints (6). In addition, compute the type of the violation, i.e., $u_{BND,i} = u_{\max}$ or $u_{BND,i} = u_{\min}$ (compare Fig. 10).

Set $t_{f,0} := a$, $\tau_{l,m+1} := b$.

If $m = 0$ then $u_{opt} := u^*$ and stop.

Step 2: Compute the lower bound $\tau_{f,i}$ of τ_i for $i = 1, \dots, m$ by the backward integration of the initial value problem (IVP)

$$\dot{y} = g(y, u, t), \quad u = u_{BND,i}, \quad y(t_{f,i}) = y^*(t_{f,i}) \quad (76)$$

until the stopping condition $y(t) = y^*(t)$. This determines $\tau_{f,i} := t$.

Set the number of subproblems $N_{OPT} := m$ and the dimension of the i -th subproblem $N_{DIM,i} := 1$.

Step 3: For $i = 1, \dots, N_{OPT}$, the minimization subproblem of the dimension $N_{DIM,i} = 1$ to determine τ_1, \dots, τ_m has to be solved

$$\min_{\tau_i} v(\tau_{l,i+1}) = \min_{\tau_i} \int_{t_{f,i-1}}^{\tau_{l,i+1}} L(y(s), u(s), s) ds, \quad (77)$$

where v is determined by the forward integration of

$$\dot{v} = -u(t)y(t), \quad v(t_{f,i-1}) = 0, \quad (78)$$

$$\dot{y} = g(y, u, t), \quad y(t_{f,i-1}) = y^*(t_{f,i-1}), \quad (79)$$

$$\text{with } u = \begin{cases} u^*, & \text{if } t_{f,i-1} \leq t < \tau_i, \\ u_{BND,i}, & \text{if } \tau_i \leq t < t_i(\tau_i), \\ u^*, & \text{if } t_i(\tau_i) \leq t \leq \tau_{l,i+1}, \end{cases} \quad (80)$$

where $t_i(\tau_i)$ is determined as follows:

Find the first zero \hat{t}_i of $y(t) = y^*(t)$ satisfying $\hat{t}_i \geq t_{f,i}$.

If $\hat{t}_i > \tau_{l,i+1}$ or if no zero exists then let $t_i := \tau_{l,i+1}$ else let $t_i := \hat{t}_i$.

Step 4: Convergence check 1 by comparing the subproblems i and $i + 1$ for $i = 1, \dots, N_{OPT} - 1$:

If $t_j(\tau_j) > \tau_{j+1}$ with $j(i) := \sum_{k=1}^i N_{DIM,k}$

then combine the two subproblems i and $i + 1$ to a new subproblem of dimension $N_{DIM,i} + N_{DIM,i+1}$.

Convergence check 2 for bang-bang points in each subproblem

for $i = 1, \dots, N_{OPT}$:

If $y(\tau_k)$ violates Lemma 2 for a $k = l(i) + 2, \dots, j(i)$ with $l(i) := \sum_{k=1}^{i-1} N_{DIM,k}$ then decouple the subproblem i into two new subproblems of dimensions $k - l(i) - 1$ and $j(i) - k + 1$.

If no subproblem has been modified then u_{opt} is determined by τ_1, \dots, τ_m , stop, else adjust N_{OPT} and $N_{DIM,i}$ and go to Step 5.

Step 5: Solve the new generated minimization subproblems

$$\min_{\tau_{l(i)+1}, \dots, \tau_{j(i)}} v(\tau_{j(i)+1}), \tag{81}$$

where v is determined by the forward integration of

$$\dot{v} = -u(t)y(t), \quad v(t_{f,l(i)}) = 0, \tag{82}$$

$$\dot{y} = g(y, u, t), \quad y(t_{f,l(i)}) = y^*(t_{f,l(i)}), \tag{83}$$

$$\text{with } u = \begin{cases} u^*, & \text{if } t_{f,l(i)} \leq t < \tau_{l(i)+1}, \\ u_{BND,l(i)+1}, & \text{if } \tau_{l(i)+1} \leq t < \tau_{l(i)+2}, \\ \dots & \\ u_{BND,j(i)}, & \text{if } \tau_{j(i)} \leq t < t_{j(i)}(\tau_{j(i)}) \\ u^*, & \text{if } t_{j(i)}(\tau_{j(i)}) \leq t \leq \tau_{l,j(i)+1}, \end{cases} \tag{84}$$

where $t_{j(i)}(\tau_{j(i)})$ is determined as follows with $j = j(i)$:

Find the first zero \hat{t}_j of $y(t) = y^*(t)$ satisfying $\hat{t}_j \geq t_{f,j}$.

If $\hat{t}_j > \tau_{l,j+1}$ or if no zero exists then let $t_j := \tau_{l,j+1}$ else let $t_j := \hat{t}_j$.

Go back to Step 4.

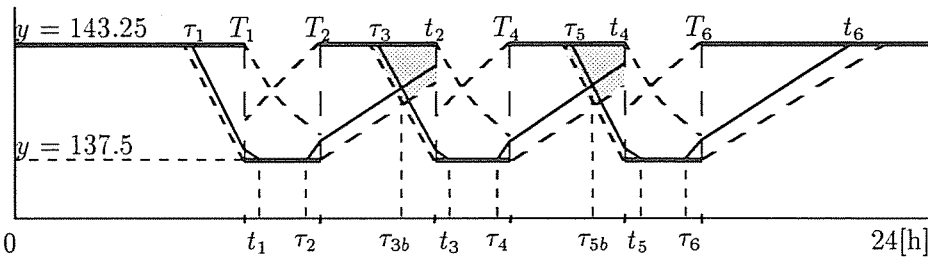


Figure 6

The qualitative behaviour of the solution of Step 3 is shown in Fig. 6 for the three-peak model. Here y^* is a piecewise constant function and takes the values 143.25 and 137.5 (bold lines). There, the control u^* does not violate its bounds in the interior of each piecewise constant arc of y^* . However, at the six discontinuities of y^* the singular control takes the values $u^*(T_{2i-1}) = +\infty, u^*(T_{2i}) = -\infty, i = 1, 2, 3$ (Dirac function). Here, the 6 intervals where u^* violates its bounds are reduced to points: $[\tau_{l,i}, t_{f,i}] = [T_i, T_i], i = 1, \dots, 6$ (for a continuous influx $Z(t)$ this case cannot happen). Therefore, we have to solve 6 one dimensional optimization problems in Step 3 to determine a first estimate of $\tau_i, i = 1, \dots, 6$. The solutions behave as the thin solid curves.

These six curves show two intersections at τ_{3b} and τ_{5b} in the dotted areas. This indicates that there might exist two bang-bang points.

In *Step 4* of the algorithm, the subproblems 2 and 3, and 4 and 5, respectively, are merged together. Thus, $N_{OPT} := 4$ and $N_{DIM,1} = N_{DIM,4} = 1$, $N_{DIM,2} = N_{DIM,3} = 2$. In *Step 5*, the newly generated subproblems 2 and 3 are solved to obtain the optimal control (cf. Fig. 7).

Some implementation details of the Real-Time-Optimization algorithm, RTOPT, are

1. The numerical integration of the IVPs can be performed by any appropriate method, e.g., the extrapolation code DIFSYS based on Bulirsch, Stoer [2]. For the IVPs with stopping conditions, an appropriate method with root finding must be used, e.g., the multistep and variable order method LSODAR due to Hindmarsh [8] and Petzold [9].
2. A high relative accuracy of the numerical integration, for example 10^{-12} , is required to determine the roots $t_i(\tau_i)$ sufficiently accurately.
3. For the numerical integration of the IVPs, stopping points have to be considered in order to avoid order reduction and inefficiency of the integration methods. These stopping points result from a piecewise definition of the model functions, e.g., the influx of water $Z(t)$.
4. The SQP-method NPSOL due to Gill, Murray, Saunders, Wright [5], Version from NAG library Mark 14, is used with finite difference gradients for the minimization with simple bounds on the variables. The relative precision in the objective value is required to be 10^{-8} . Round-off, truncation, and integration error have to be considered when calculating suitable steplengths for finite difference gradients [4].
5. Initial estimates of the τ_i are chosen within the interval $]\tau_{f,i}, \tau_{i,i}[$.

5. Numerical Results

All calculations were performed on a CDC Cyber 995 in single precision (48 bit mantissa). The reported computing times are about 3 times faster than on a 80486 PC with 33 Mhz in double precision.

The influx of water $Z(t)$ is periodic function with a period of 24h and so is the solution. For convenience, algorithm RTOPT is therefore applied to the time interval $[2h, 26h]$ instead of $[0h, 24h]$ to have all the switching points τ_i and t_i in the considered interval (cf. Table 1).

5.1 The Three-Peak Model

For this problem, the optimal solution can also be obtained analytically. Here we used the symbolic computation system MAPLE [3]. The exact results are shown in Table 1. The optimal energy production is 821.2900935 [MWh].

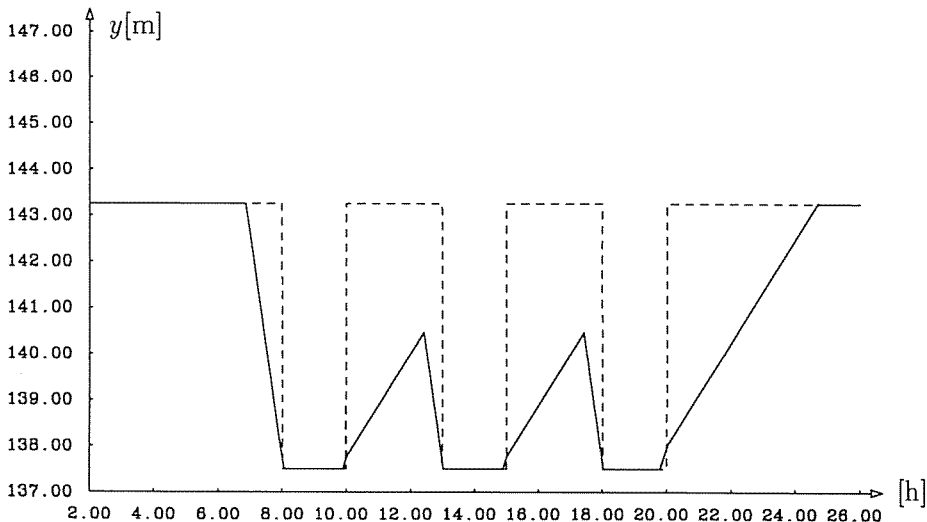
Table 1. Solution data of the three-peak model

i	1	2	3	4	5	6
τ_i	6.859089127	9.89112946	12.41574871	14.89112946	17.41574871	19.78947289
$y(\tau_i)$	143.2500000	137.5000000	140.4440989	137.5000000	140.4440989	137.5000000
t_i	8.052248882	—	13.02670845	—	18.02670845	24.72634283
T_i	8.000000000	10.0000000	13.00000000	15.0000000	18.00000000	20.00000000
$y(T_i)$	137.6968476	137.7410720	137.6003740	137.7410720	137.6003740	137.9616056

In [1], two different methods have been used resulting in energy production values of 821.09 [MWh] and 821.26 [MWh]. The first method of [1], has limited accuracy and the second method was reported to need too much computing time.

When applying algorithm RTOPT, the energy production obtained is 821.284 [MWh] which is very close to the exact value. The computing time is 8.3 seconds which is negligible with respect to the time interval of 24 hours. The computed switching points τ_i and the roots $t_i(\tau_i)$ are accurate up to 5 or 6 digits. In Figs. 7 and 8, the solid lines refer to the optimal filling level and the optimal control, respectively. The dashed lines refer to y^* and the associated singular control u^* , both as step functions.

In a second simulation, RTOPT is applied to the three-peak model with the smooth influx $Z_R(t)$. The obtained energy production is 822.228 [MWh] and the computing time increases to 41 seconds.

**Figure 7.** Optimal filling level of the three-peak model

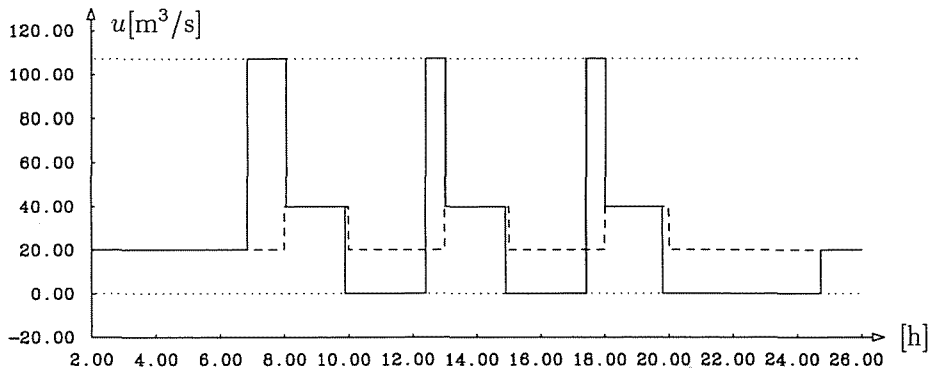


Figure 8. Optimal control of the three-peak model

5.2 The Refined Three-Peak Model

When applied to the refined model, RTOPT converges after 51 seconds with an energy production of 847.721 [MWh] and the data shown in Table 2.

In Figs. 9 and 10, the solid lines refer to the optimal filling level and the optimal control, respectively. The dashed lines refer to y^* and the associated singular control u^* .

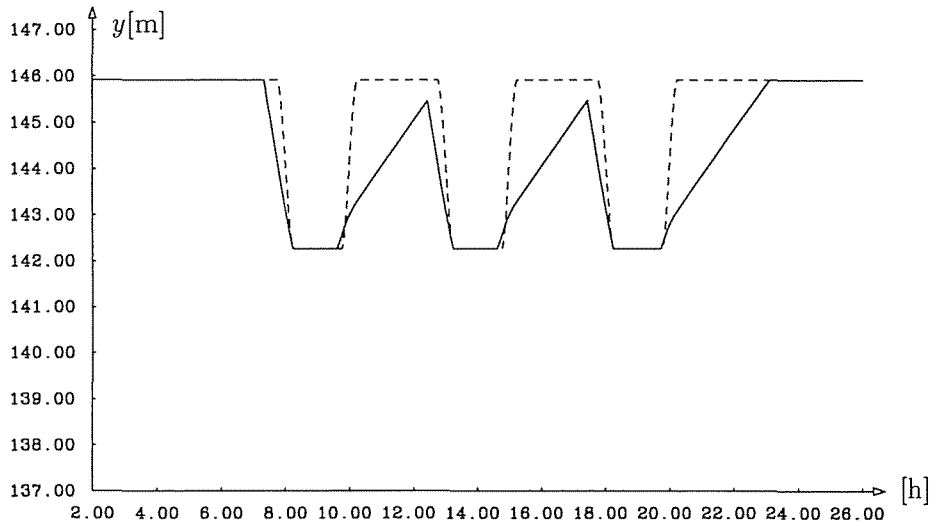


Figure 9. Optimal filling level of the refined three-peak model

Remark: The results of the two hydroelectric power plant problems show, that it is advantageous to use the whole water influx, i.e., $y(t) \leq y^*(t)$, instead of increasing

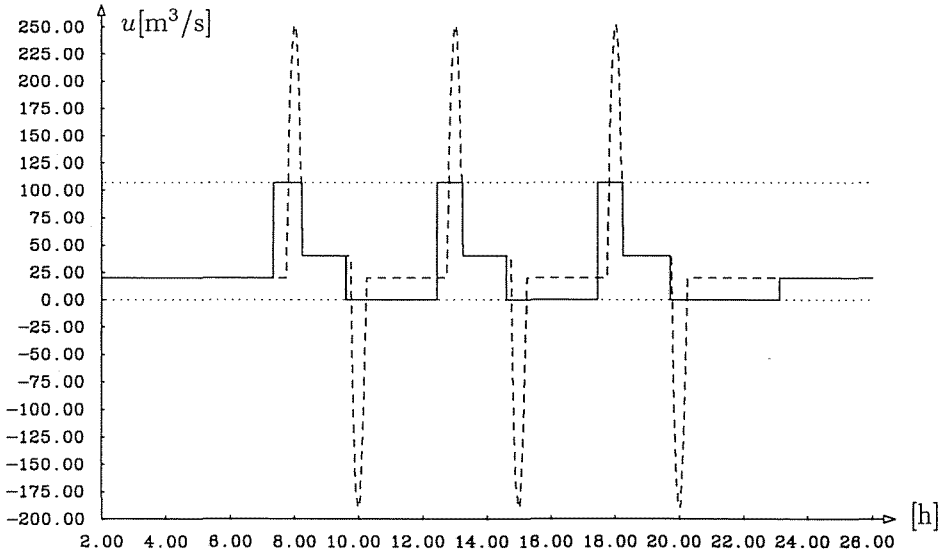


Figure 10. Optimal control of the refined three-peak model

Table 2. Solution data of the refined model

i	1	2	3	4	5	6
τ_i	7.3341236	9.6099982	12.440562	14.608938	17.440201	19.717736
$y(\tau_i)$	145.91858	142.26346	145.46530	142.26346	145.46750	142.26346
t_i	8.2297217	—	13.226839	—	18.229337	23.113114
$\tau_{f,i}$	7.3319247	8.2115025	12.331925	13.211503	17.331925	18.211502
$\tau_{l,i}$	7.8086720	9.7719729	12.808672	14.771973	17.808672	19.771973

the filling level to a value greater than $y^*(t)$. As a good approximation, we can therefore use $\tau_i = \tau_{f,i}$, if u switches to u_{\max} , and $\tau_i = \tau_{l,i}$, if u switches to u_{\min} . This suboptimal trajectory then corresponds to the lower bound of the tubes considered in Fig. 5 of Sec. 3.1. For the three-peak model, this suboptimal control yields an energy production of 820.819 [MWh] which is close to the optimal value. The difference may be larger for other model functions with different $I(y)$ and $W(y)$.

6. Conclusions

The main difficulties in the solution of the hydroelectric power plant models presented in this paper are caused by model functions that are not differentiable along the optimal trajectory.

An algorithm has been developed to compute the optimal flow of water through the turbines and the optimal filling level of the storage. By dividing the full problem into several lower dimensional subproblems, it is possible to compute the optimal solution with high accuracy in real time. Moreover, it is possible to compute the optimal solution for a long time period, as, e.g., one day or one year, knowing the influx of water only a few hours in advance.

The algorithm is also applicable to more general characteristic functions of this hydroelectric power plant model.

A further refinement of the hydroelectric power plant has to take into account the price of electricity or the demand on electricity depending on the day time. We therefore have to modify the functional by a time dependent cost function $c(t)$

$$\min_u - \int_0^T c(t)y(t)u(t) dt.$$

The strategy developed in this paper is also applicable in this case.

Acknowledgement

The authors gratefully remember the generous willingness of Prof. Dr. Hj. Wacker in making data and reports available to them [11]. The authors are also indebted to the numerical analysis group of Prof. Dr. R. Bulirsch for helpful discussions especially to Dr. K.-D. Reinsch who originally has initiated the author's investigation of the problem and to Priv.-Doz. Dr. H.-J. Pesch who has carefully read the manuscript.

References

- [1] Bauer, W., Reisinger, H., Wacker, Hj.: Höhensteuerung eines Tagesspeicherkraftwerks. *Zeitschrift f. Operations Res.* 26, B145–B167 (1982).
- [2] Bulirsch, R., Stoer, J.: Numerical treatment of ordinary differential equations by extrapolation methods. *Num. Math.* 8, 1–13 (1966).
- [3] Char, B. W., Geddes, K. O., Gonnet, G. H., Leong, B. L., Monagan, M. B., Watt, S. M.: *Maple V, language reference manual*. New York, Berlin, Heidelberg: Springer 1991.
- [4] Gill, P. E., Murray, W., Saunders, M. A., Wright, M. H.: Computing forward-difference intervals for numerical optimization. *SIAM J. Sci. Stat. Comput.* 4, 310–321 (1983).
- [5] Gill, P. E., Murray, W., Saunders, M. A., Wright, M. H.: *User's guide for NPSOL (Version 4.0)*. Report SOL 86-2, Department of Operations Research, Stanford University, California, USA, 1986.
- [6] Engl, H. W.: In memoriam Hansjörg Wacker. *Computing* 46, 275–278 (1991).
- [7] Hestenes, M. R.: *Calculus of variations and optimal control theory*. New York, London, Sydney: J. Wiley & Sons 1966.
- [8] Hindmarsh, A. C.: ODEPACK, a systemized collection of ode solvers. In: Stepleman, R. S. et al. (eds.) *Scientific computing*. Amsterdam: North Holland 1983, pp. 55–64.
- [9] Petzold, L. R.: Automatic selection of methods for solving stiff and nonstiff systems of ordinary differential equations. *SIAM J. Sci. Stat. Comput.* 4, 136–148 (1983).
- [10] Stoer, J., Bulirsch, R.: *Introduction to numerical analysis*, 2nd ed. Berlin, Heidelberg, New York: Springer 1983.
- [11] Wacker, Hj.: Private communication. April, 1990.

- [12] Wacker, Hj., Ottendörfer, W., Buchinger, S., Zarzer, E., Zieba, A., Eder, Bauer, Rathmeier, Gollmann, Haider, Takacs, Eiblhuber: Optimierung bei der Hydroenergiegewinnung, Teil I: Modell. Preprint Nr. 158, Math. Inst., Joh. Kepler Univ. of Linz, Linz, Austria, 1980.

Dr. rer. nat. Martin Kiehl
Dipl. Math. Oskar von Stryk
Mathematisches Institut
Technische Universität München
Postfach 20 24 20
D-W-8000 München 2
Federal Republic of Germany